

High Performance Repetitive Control of an Active Filter under Varying Network Frequency^{*}

Ramon Costa-Castelló, Shane Malo, Robert Griño

*Institut d'Organització i Control de Sistemes Industrials (IOC),
Universitat Politècnica de Catalunya (UPC), Barcelona, Spain,
(e-mail: {ramon.costa, shane.malo, roberto.grino}@upc.edu).*

Abstract: Shunt active power filters are power electronics devices that are connected in parallel with nonlinear and reactive loads to compensate these characteristics in order to assure the quality of service of the electrical distribution network. This work proposes and designs a controller, based on combined feedforward and feedback actions, the last using repetitive control, to obtain a good closed-loop performance (power factor close to 1 and, load current harmonics and reactive power compensation) in spite of the possible frequency variations that may occur in the electrical network. It is known that these variations clearly affect the performance of the usual discrete-time implementations of the repetitive based controllers. This work analyzes the effect of these variations and describes the architecture of the controller, its design, and the mechanism to compensate the network frequency variations. Some experimental results that show the good performance of the closed-loop system are also included.

Keywords: Active power filters, current harmonics compensation, reactive power compensation, repetitive control, digital control implementation

1. INTRODUCTION

Active filters are devices which allow to coexist nonlinear loads and good energy quality in distribution networks. A main effort in the design and control of these devices has been carried out in the past years. One research line deals with topologies and architectures, see for example (Akagi [1996], El-Habrouk et al. [2000], Salo and Tuusa [2005]): several types of topologies have been proposed including parallel (shunt active filters), serial and hybrid serial-parallel connections, mixed passive-active devices and converter based active filters with voltage or current dc bus. Another important research line is the control of active filters, where many approaches have been proposed (Wu and Jou [1996], Choi [2005], Buso et al. [1998], Mattavelli [2001], Singh et al. [1998]). Most of them are based on two hierarchical control loops, an inner one in charge of assuring the desired current and an outer one in charge of determining the required shape as well as the appropriate power balance. The current control loop needs to be fast and precise in order to assure the desired energy flow quality. In this sense, an approach which has proved to be specially efficient is repetitive control. This control technique is based on the Internal Model Principle (Francis and Wonham [1976]) which allows the design of a controller capable of rejecting or tracking periodic signals in steady state (Costa-Castelló et al. [2004], Costa-Castello et al. [2005]). However, repetitive controllers are

designed for a predefined frequency¹ and, unfortunately, when this frequency slightly changes the tracking/rejecting capabilities decay dramatically.

In order to overcome this problem several approaches, that can be grouped in two main areas, have been proposed: to preserve the sampling time (Steinbuch [2002], Cao and Ledwich [2002]) or to change it adaptively (Liu and Yang [2004], Manayathara et al. [1996], Hillerström and Sternby [1994]). For the first approach there are also two main ideas: improving robustness by using large memory elements (Steinbuch [2002]) or introducing a fictitious sampler operating at a variable sampling rate and later using a fixed frequency internal model (Cao and Ledwich [2002]). These two ideas improve the performance of the system for small frequency variations but increase the computational burden. An alternative approach is to adapt the controller sampling rate according to the disturbance/reference period (Hillerström and Sternby [1994], Manayathara et al. [1996], Liu and Yang [2004]). This allows to preserve the steady-state performance while maintaining a low computational cost but, on the other hand, it implies structural changes in the system behavior which may destabilize the closed-loop system.

The controller designed in this work uses the traditional two control loops decomposition. The current controller is composed by a feedforward action in charge of assuring very fast transient response and a feedback control law in charge of assuring closed-loop stability and a very good harmonic correction performance. The feedback control

^{*} This work was supported in part by the Spanish *Ministerio de Educación y Ciencia* under project DPI2007-62582.

¹ Once the sampling period is fixed this frequency is structurally embedded in the control algorithm.

law is based on the use of a repetitive odd-harmonic controller (Griñó and Costa-Castelló [2005]). The outer control law is based on the exact computation of the sinusoidal current network amplitude and, in order to improve robustness, this computation is combined with a feedback control law with an analytically tuned PI controller. Both the inner and the outer loop adapt their sampling frequency to the period of the signal being tracked. This adaptive procedure combined with the introduction of feedforward paths are the main contributions of this work and yield very good performance both in transient and in steady-state behavior and robustness in front of network frequency variations.

2. PROBLEM FORMULATION

2.1 Physical model of the boost converter

Fig. 1 presents the system architecture. A load is connected to the power source, in parallel an active filter is applied in order to fulfill the desired behavior, i.e. to guarantee unity power factor at the network side. A boost converter with the ac neutral wire connected directly to the midpoint of the dc bus is used as active filter. The averaged (at the switching frequency) model of the boost converter is given by

$$L \frac{di_f}{dt} = -r_L i_f - v_1 d - v_2 (d - 1) + v_n \quad (1)$$

$$C_1 \frac{dv_1}{dt} = -\frac{v_1}{r_{C,1}} + i_f d \quad (2)$$

$$C_2 \frac{dv_2}{dt} = -\frac{v_2}{r_{C,2}} + i_f (d - 1) \quad (3)$$

where d is the duty ratio, i_f is the inductor current and v_1, v_2 are the dc capacitor voltages, respectively; $v_n = V_n \sqrt{2} \sin(\omega_n t)$ is the voltage source²; L is the converter inductor, r_L is the inductor parasitic resistance, C_1, C_2 are the converter capacitors and $r_{C,1}, r_{C,2}$ are the parasitic resistances of the capacitors. The control variable, d , takes its value in the closed real interval $[0, 1]$ and represents the averaged value of the PWM (pulse-width modulation) control signal injected to the actual system.

Due to the nature of the voltage source, the load current, in steady-state, is usually a periodic signal with only odd-harmonics in its Fourier series expansion, so the current can be written as $i_l = \sum_{n=0}^{\infty} a_n \sin(\omega_n (2n + 1) t) + b_n \cos(\omega_n (2n + 1) t)$, where $a_n, b_n \in \mathbb{R}$ are the real Fourier series coefficients of the load current.

2.2 Control objectives

The active filter goal is to assure that the load is seen as a resistive one. This goal can be stated as $i_n^* = I_d^* \sin(\omega_n t)$, i.e. the source current must have a sinusoidal shape in phase with the network voltage³. Another collateral goal, necessary for a correct operation of the converter, is to assure constant average value of the dc bus voltage⁴, i.e. $\langle v_1 + v_2 \rangle_0^* = v_d$, where v_d must fulfill the boost

² $\omega_n = 2\pi/T_p$ rad/s is the network frequency.

³ x^* represents the steady-state value of signal $x(t)$.

⁴ $\langle x \rangle_0$ means the dc value, or mean value, of the signal $x(t)$.

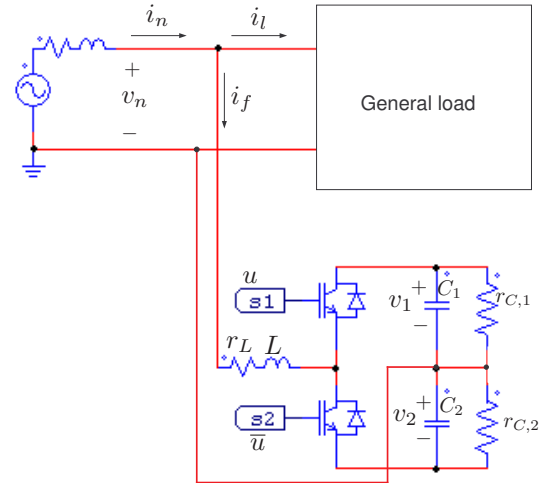


Fig. 1. Single-phase shunt active filter connected to the network-load system.

condition ($v_d > 2\sqrt{2}v_n$). It would be also desirable that this voltage would be almost equally distributed among both capacitors ($v_1 \approx v_2$).

2.3 Rewriting the plant equations

It is standard for this kind of systems to linearize the current dynamics by the partial state feedback $\alpha = v_1 d + v_2 (d - 1)$. Moreover, the change of variables $i_f = i_f$, $E_C = \frac{1}{2} (C_1 v_1^2 + C_2 v_2^2)$, $D = C_1 v_1 - C_2 v_2$ makes two more meaningful variables appear. Namely, E_C , the energy stored in the converter capacitors and D , the charge unbalance between them. Assuming that the two dc bus capacitors are equal ($C = C_1 = C_2$, $r_C = r_{C,1} = r_{C,2}$) the system dynamics using the new variables is

$$L \frac{di_f}{dt} = -r_L i_f + v_n - \alpha \quad (4)$$

$$\frac{dE_C}{dt} = -\frac{2E_C}{r_C C} + i_f \alpha \quad (5)$$

$$\frac{dD}{dt} = -\frac{1}{r_C C} D + i_f \quad (6)$$

It is important to note that (4) and (6) are linear and decoupled with respect to state variable E_C . The partial state feedback and the change of variables will be applied as the lowest level control action on the closed-loop system.

3. CONTROL DESIGN

The controller is designed using a two level approach: first, an inner current controller which forces the sine wave shape for the network current and, second, an outer control loop to fulfill the appropriate active power balance for the whole system. The output of this loop is the amplitude of the sinusoidal reference for the current control loop. The active power balance is achieved if the energy stored in the active filter capacitors, E_C , is equal to a reference value, E_C^d .

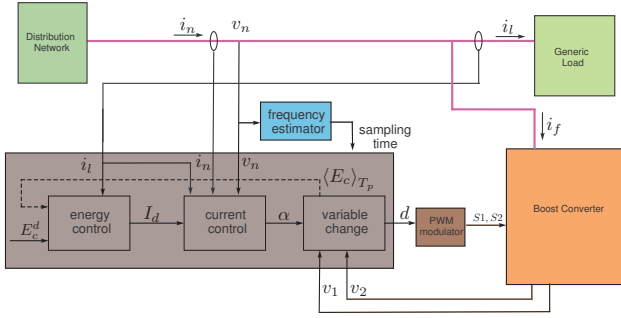


Fig. 2. Global architecture of the control system.

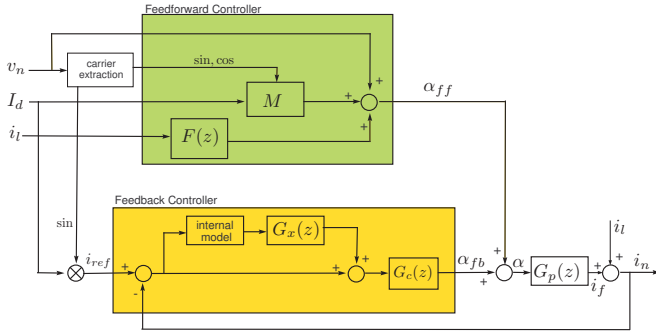


Fig. 3. Current control block diagram.

3.1 Current loop controller

Taking benefit from the fact that (4) is linear, a linear controller is designed to force a sinusoidal shape in i_n . This controller consists of two parts, see Fig. 3:

- A feedforward controller which fixes the desired steady state:
$$i_n^* = I_d^* \sin(\omega_n t) \quad (7)$$
- A feedback controller which compensates uncertainties and assures closed-loop stability.

As previously stated, the current control goal is to assure that $i_n^* = I_d^* \sin(\omega_n t) = i_f(t) + i_l(t)$, where I_d^* is constant in steady state. From to circuit topology and (4)

$$\frac{di_n}{dt} = -\frac{r_L i_n}{L} - \frac{\alpha}{L} + \frac{v_n}{L} + \frac{di_l}{dt} + \frac{r_L i_l}{L} \quad (8)$$

In order to force i_n to the desired value given in (7) it is necessary that α takes the value

$$\begin{aligned} \alpha_{ff} &= v_n + \left(L \frac{d}{dt} + r_L \right) i_l - (r_L \sin(\omega_n t) + L\omega_n \cos(\omega_n t)) I_d \\ &= v_n + F(i_l) + M(I_d, t, \omega_n) \end{aligned} \quad (9)$$

thus defining the nominal control action that will keep the system in the desired trajectory, so it will be used as a feedforward action. As the system will have a digital implementation F will be approximated as $F(z) = \frac{(L+T_s r_L)z-L}{T_s z}$. This action will be combined with a feedback controller to overcome model uncertainties, disturbances and measurement noise.

The dynamics of (4) once transformed to discrete time can be written as

$$G_p(z) = \frac{I_f(z)}{\alpha(z)} = \frac{\left(1 - e^{-\frac{r_L T_s}{L}}\right) \frac{1}{r_L}}{z - e^{-\frac{r_L T_s}{L}}} \quad (10)$$

As the signal to be tracked and rejected in this system is an odd-harmonic periodic one, it is convenient to design a controller which allows to track and to reject this type of signal. A technique which has been proved to be specially suitable for this type of signals is repetitive control (Inoue et al. [1981]) and, in particular, odd-harmonic repetitive control (Griño and Costa-Castelló [2005]).

Repetitive controllers are composed by an internal model which assures steady-state performance and a stabilizing controller, $G_x(z)$, which assures closed-loop stability. Traditionally, repetitive controllers are implemented in a “plug-in” fashion, i.e. the repetitive compensator is used to augment an existing nominal controller, $G_c(z)$ (Fig. 3). This nominal compensator is designed to stabilize the plant, $G_p(z)$, and provides disturbance attenuation across a broad frequency spectrum. The internal model used in odd-harmonic repetitive control (Griño and Costa-Castelló [2005]) has the form $\frac{-H(z)}{z^{\frac{N}{2}} + H(z)}$, where $N = \frac{T_p}{T_s}$ and $H(z)$ is a low pass filter used to improve system robustness. It is important to note that N corresponds to the discrete-time period of the signal to be tracked/rejected and its value is structurally introduced in the control system. In this work the values $T_p = \frac{1}{50}$ s and $N = 400$ have been selected to obtain a good reconstruction of the continuous-time signals.

The closed-loop system of Fig. 3 is stable if the following conditions are fulfilled (Griño and Costa-Castelló [2005]):

- (1) The closed loop system without the repetitive controller is stable, i.e. $G_o(z) = \frac{G_c(z)G_p(z)}{1+G_c(z)G_p(z)}$ is stable. It is advisable to design the controller $G_c(z)$ with a high enough robustness margin so, in this work, the lag controller $G_c(z) = -\frac{0.6305z-0.629}{z-0.9985}$ which provides a phase margin of 140° has been used.
- (2) $\|H(z)\|_\infty < 1$. $H(z)$ is designed to have gain close to 1 in the desired bandwidth and attenuate the gain out of it. The first order linear-phase FIR filter $H(z) = \frac{1}{4} \cdot z + \frac{1}{2} + \frac{1}{4} \cdot z^{-1}$ has proved to be good enough in this application.
- (3) $\|1 - G_o(z)G_x(z)\|_\infty < 1$, where $G_x(z)$ is a design filter to be chosen. A trivial structure⁵ which is often used is (Tomizuka et al. [1989]): $G_x(z) = k_r (G_o(z))^{-1}$. As argued in Hillerström and Lee [1997], k_r must be designed looking for a trade-off between robustness and transient response. In this application $k_r = 0.3$ has been selected.

The repetitive controller defines the feedback law

$$\alpha_{fb} = G_c(z) \left(1 + G_x(z) \left(\frac{-z^{-N/2} H(z)}{1 + z^{-N/2} H(z)} \right) \right) (i_{ref} - i_n)$$

that will be used with the feedforward action given in (9) thus giving $\alpha = \alpha_{fb} + \alpha_{ff}$. Fig. 3 shows the complete current control loop that will be used in the system.

Under the combined action of the feedforward and the feedback control action, the network current can be assumed to be $i_n(t) \approx I_d(t) \sin(\omega_n t)$ that, from now on, will be taken as a fact.

⁵ There is no problem with the improperness of $G_x(z)$ because the internal model provides the repetitive controller with a high positive relative degree.

3.2 Energy shaping (voltage loop) controller

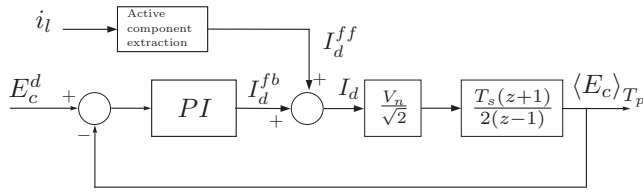


Fig. 4. Simplified 50Hz energy (voltage) control loop.

Following the developments in Costa-Castelló et al. [2007], the outer controller that assures a mean value⁶ of the energy stored in the capacitors, $\langle E_c(t) \rangle_{T_p}$ close to the desired reference value, E_c^d is made up of two parts (see Fig. 4):

- A feedforward term which makes $I_d^{ff} = a_0$. This feedforward term assures the energy balance in the ideal case ($r_L = 0$ and $r_C = 0$) and takes into account i_l characteristics and changes instantaneously. I_d^{ff} is calculated using an amplitude modulator with a scaled signal of the source voltage as a carrier and a mean value extraction. This last operation has been implemented as the filter $P(z) = \frac{1}{N} \frac{1-z^{-N}}{1-z^{-1}}$ which corresponds to a good approximation of the corresponding continuous-time mean value extraction operation.
- A feedback term which is in charge of compensating dissipative effects and the system uncertainties.

The dynamics of the plant can be modeled by the discrete-time integrator $\frac{T_s(z+1)}{2(z-1)}$ and the losses in the inductor and capacitors parasitic resistances can be considered as an additive disturbance. So, the PI controller

$$I_d^{fb} = k_i \frac{T_s(z+1)}{2(z-1)} \Delta E + k_p \Delta E, \quad (11)$$

where $\Delta E = E_c^d - \langle E_c(t) \rangle_{T_p}$, will regulate $\langle E_c(t) \rangle_{T_p}$ to the desired value E_c^d without steady-state error.

3.3 Period (T_p) variations

Most control algorithms in the previous section contain the value N , this parameter corresponds to the discrete-time period $N = \frac{T_p}{T_s}$ of the periodic signals to be tracked or attenuated. In systems, in which the period of the signal is kept constant, N and T_s are designed a priori according to the desired number of samples per period and the technological constrains over T_s . However, in this case, the electrical distribution network frequency can suffer from fluctuations and, then, T_p can not be assumed constant.

If the period T_p varies, the value of N or T_s should be changed in order to preserve the relationship $N = T_p/T_s$. If this is not the case the control algorithm performance may drastically decay. As an example, Fig. 5 show the feedback control open-loop gain designed for a nominal frequency of 50Hz with the gain for 49Hz, 50Hz and 51Hz (and some of their harmonics) highlighted. Note that while for the 50Hz signal the gain is important it decays for

⁶ $\langle f(t) \rangle_{T_p} = \frac{1}{T_p} \int_{t-T_p}^t f(\tau) d\tau$.

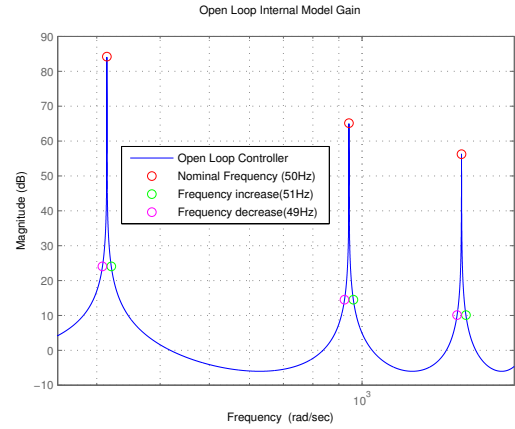


Fig. 5. Open-loop transfer function gain diagram.

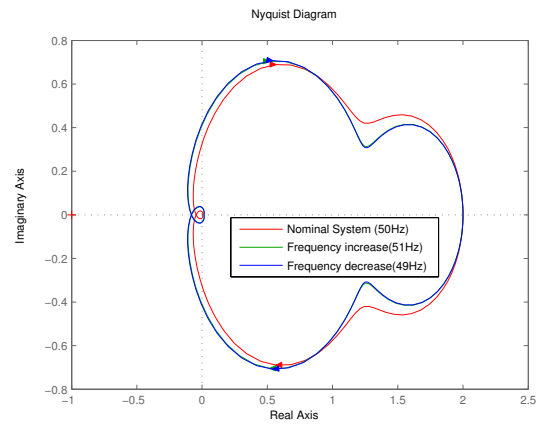


Fig. 6. Open-Loop transfer function $G_c(z)G_p(z)$ Nyquist plot (the closed-loop system is stable in all cases).

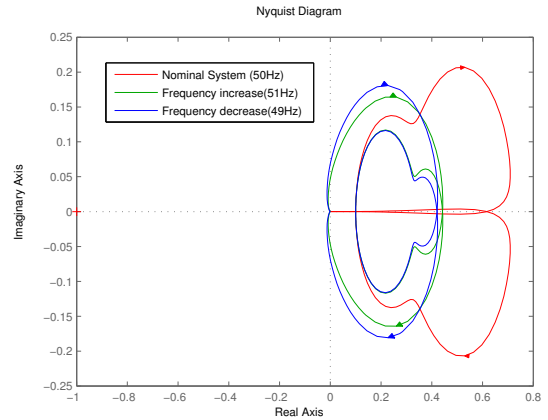


Fig. 7. Nyquist plot of $1 - G_o(z)G_x(z)$ for different values of T_s .

the other frequencies. Something similar occurs with the phase lag of the closed-loop control system. While for the nominal frequency the phase is almost zero this is not true for the other frequencies. It is important to emphasize that, in the particular case of the active filter, this would imply a reduction of the harmonic rejection capabilities and the introduction of reactive current in the system. Clearly, both effects would contribute to the reduction of the system performance. To overcome this problem in this work the sample time T_s will be adaptively varied in order

to satisfy the abovementioned relationship and, therefore, to maintain N constant.

However, the change of T_s implies changes in the system dynamics and, particularly in the plant model, $G_p(z)$. It is important to check that these changes does not imply a loss of closed-loop stability. This property can be checked using conditions 1, 2 and 3 in Section 3.1. Condition 1 is satisfied if the closed-loop system without the repetitive controller is stable. This condition can be checked by verifying the stability for each value of T_s . Fig. 6 shows the Nyquist plot of the open-loop transfer function $G_c(z)G_p(z)$ for different values of the sampling rate. It can be seen that the closed-loop system will be stable for all of them within the interest range. Condition 2 is always fulfilled because it does not depend on T_s . And, finally, Condition 3 is checked by inspection of Fig. 7 which shows that all the plots stay within the unitary circle so, all of them will satisfy $\|1 - G_o(z)G_x(z)\|_\infty < 1$ which implies closed-loop stability. As a conclusion, it can be stated that the closed-loop system will be stable for all the values of T_s in the interest interval. Besides this, as the network frequency varies very slowly this type of test is enough.

4. EXPERIMENTAL SETUP AND RESULTS

4.1 Experimental setup

The experimental setup is composed by a controlled dc-ac converter, that acts as a variable frequency ac source⁸, a full-bridge diode rectifier (nonlinear load) and the previously described single-phase active filter. Between the dc-ac converter and the rectifier there is an inductor to simulate a real ac source with a non negligible output impedance. The active filter is connected in a shunt manner with the rectifier to compensate its distorted current.

The active filter controller has been implemented on a DSP based hardware, so all the controller is implemented in a digital framework, with a nominal sampling frequency equal to the switching frequency of 20 kHz. The network frequency is obtained from the network voltage zero crossings through some additional hardware and a digital lowpass filter that runs in the DSP as shown in Fig. 8. With this information the sampling frequency is updated to maintain the ratio $N = 400$.

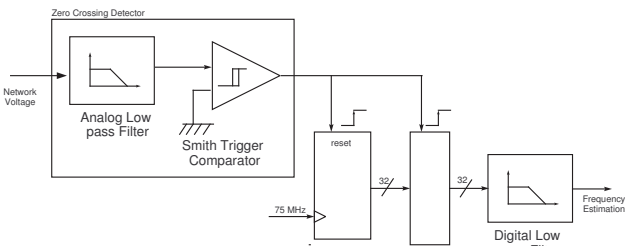


Fig. 8. Network frequency computation.

⁷ Note that the controller is not affected by the sampling rate.

⁸ This source emulates a poor frequency controlled grid or a combustion engine generator.

4.2 Experimental results

Fig. 9 shows the waveforms⁹ of v_n and i_n when the nonlinear load is connected to the ac source (inverter plus inductor). The rectifier current has a total harmonic distortion¹⁰ (THD) of 65.5% and induces a THD of 5.6% in v_n .

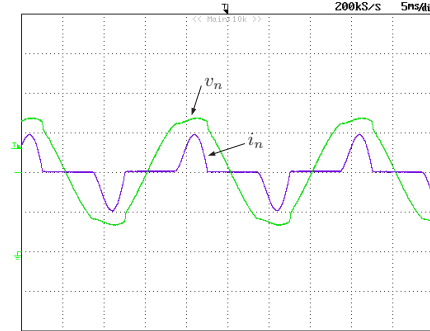


Fig. 9. v_n and i_n vs time with the nonlinear load.

As Fig. 10 shows, when the active filter is connected in parallel with the rectifier the shape of the current at the source port is nearly sinusoidal with a THD of 2.0% and, then, the source voltage recovers a non distorted shape with a THD of 0.2%. It is also worth to remark that the power factor (PF) and $\cos \phi$ at the port are unitary.

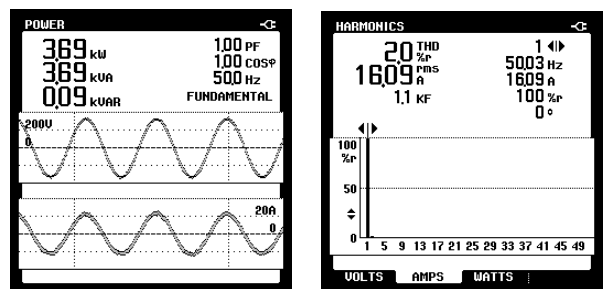
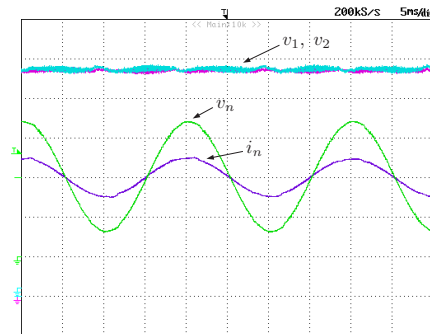


Fig. 10. Nonlinear load and the active filter at a network frequency of 50 Hz. (top) v_n , i_n and v_1, v_2 vs time; (bottom) PF, $\cos \phi$ and THD for i_n .

In the next experiment the network frequency of the system changes from 50 Hz to 52 Hz in a step manner. The response of v_n , i_n and the semibus voltages v_1, v_2 is plotted in Fig. 11 (top) and shows that, after a transient, the system reaches the steady state. Also, as the information

⁹ In Fig. 9, Fig. 10 (top) and Fig. 11 (top) the scales are: v_n (230 V/div), i_n (48 A/div) and v_1, v_2 (74,5 V/div).

¹⁰ In this work the THD is calculated with respect to the rms value of the signal.

in Fig. 11 (bottom) depicts, when the system is at steady state at 52 Hz the PF and the $\cos \phi$ return to unitary values and the THD for i_n is 2.1%.

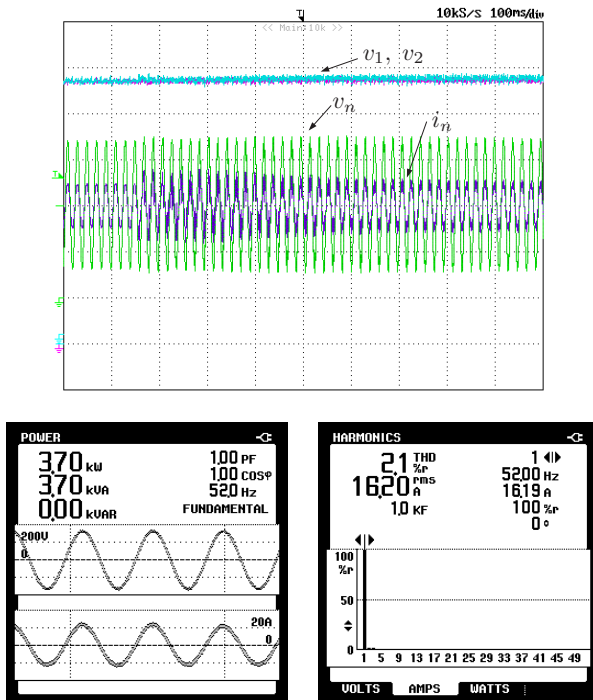


Fig. 11. Nonlinear load and the active filter. (top) v_n , i_n and v_1, v_2 vs time when the network frequency changes from 50 Hz to 52 Hz; (bottom) v_n , i_n , PF, $\cos \phi$ and THD for i_n when the system reaches the steady state at 52 Hz.

5. CONCLUSIONS

This work shows the architecture and some design issues for an active filter digital controller based on repetitive control. The controller includes a mechanism to follow the network frequency variations without losing the advantages of the repetitive control and maintaining its low computational cost. The experiments prove that the controlled system has a good performance and that, using the frequency adaptation mechanism, it is able to cope with more aggressive frequency changes than the usual ones in electrical distribution networks.

REFERENCES

H. Akagi. New trends in active filters for power conditioning. *IEEE Trans. on Industry Applications*, 32(6): 1312–1322, November 1996.

S. Buso, L. Malesani, and P. Mattavelli. Comparison of current control techniques for active filters applications. *IEEE Trans. on Industrial Electronics*, 45:722–729, October 1998.

Z. Cao and G. F. Ledwich. Adaptive repetitive control to track variable periodic signals with fixed sampling rate. *IEEE/ASME Trans. on Mechatronics*, 7(3):378–384, September 2002.

S. Choi. A three-phase unity-power-factor diode rectifier with active input current shaping. *IEEE Trans. on Industrial Electronics*, 52(6):1711–1714, December 2005.

R. Costa-Castelló, R. Griñó, and E. Fossas. Odd-harmonic digital repetitive control of a single-phase current active filter. *IEEE Trans. on Power Electronics*, 19(4):1060–1068, July 2004.

R. Costa-Castello, J. Nebot, and R. Griñó. Demonstration of the internal model principle by digital repetitive control of an educational laboratory plant. *IEEE Trans. on Education*, 48(1):73–80, February 2005.

R. Costa-Castelló, R. Griñó, R. Cardoner, and E. Fossas. High performance control of a single-phase shunt active filter. In *Proc. of the 2007 IEEE International Symposium on Industrial Electronics (ISIE 2007)*, pages 3350–3355, June 2007.

M. El-Habrouk, M.K. Darwish, and P. Mehta. Active power filters : A review. *IEE Proc. Electrical Power Applications*, 5(147):403–413, September 2000.

B.A. Francis and W.M. Wonham. Internal model principle in control theory. *Automatica*, 12:457–465, 1976.

R. Griñó and R. Costa-Castelló. Digital repetitive plug-in controller for odd-harmonic periodic references and disturbances. *Automatica*, 41(1):153–157, January 2005.

G. Hillerström and R. C.H. Lee. Trade-offs in repetitive control. Technical Report CUED/F-INFENG/TR 294, University of Cambridge, June 1997.

G. Hillerström and J. Sternby. Rejection of periodic disturbances with unknown period—a frequency domain approach. In *Proc. of the 1994 American Control Conference (ACC 1994)*, volume 2, pages 1626–1631, July 1994.

T. Inoue, M. Nakano, T. Kubo, S. Matsumoto, and H. Baba. High accuracy control of a proton synchrotron magnet power supply. In *Proc. of the 8th World Congress of IFAC*, pages 216–220, 1981.

J. Liu and Y. Yang. Frequency adaptive control technique for rejecting periodic runout. *Control Engineering Practice*, 12:31–40, 2004.

T. J. Manayathara, T. Tsao, and J. Bentsman. Rejection of unknown periodic load disturbances in continuous steel casting process using learning repetitive control approach. *IEEE Trans. on Control Systems Technology*, 4(3):259–265, May 1996.

P. Mattavelli. A closed-loop selective harmonic compensation for active filters. *IEEE Trans. on Industry Applications*, 37(1):81–89, January 2001.

M. Salo and H. Tuusa. A new control system with a control delay compensation for a current-source active power filter. *IEEE Trans. on Industrial Electronics*, 52(6):1616–1624, December 2005.

B. Singh, K. Al-Haddad, and A. Chandra. A new control approach to Three-Phase active filter for harmonics and reactive power compensation. *IEEE Trans. on Power Systems*, 13(1):133–137, February 1998.

M. Steinbuch. Repetitive control for systems with uncertain period-time. *Automatica*, 38:2103–2109, 2002.

M. Tomizuka, T. Tsao, and K. Chew. Analysis and synthesis of discrete-time repetitive controllers. *Journal of Dynamic Systems, Measurement, and Control*, 111: 353–358, September 1989.

J.C. Wu and H.L. Jou. Simplified control method for the single-phase active power filter. *IEE Proc. Electrical Power Applications*, 143(3):219–224, May 1996.